

# *K*-Shell Photoionization of B-like Oxygen ( $O^{3+}$ ) Ions: Experiment and Theory

B M McLaughlin<sup>1,2,§</sup>, J M Bizau<sup>3,4,†</sup>, D Cubaynes<sup>3,4</sup>, M M Al Shorman<sup>3</sup>, S Guilbaud<sup>3</sup>, I Sakho<sup>5</sup>, C Blancard<sup>6</sup> and M F Gharaibeh<sup>7</sup>

<sup>1</sup>Centre for Theoretical Atomic, Molecular and Optical Physics (CTAMOP), School of Mathematics and Physics, The David Bates Building, 7 College Park, Queen's University Belfast, Belfast BT7 1NN, UK

<sup>2</sup>Institute for Theoretical Atomic and Molecular Physics (ITAMP), Harvard Smithsonian Center for Astrophysics, MS-14, Cambridge, MA 02138, USA

<sup>3</sup>Institut des Sciences Moléculaires d'Orsay (ISMO), CNRS UMR 8214, Université Paris-Sud, Bât. 350, F-91405 Orsay cedex, France

<sup>4</sup>Synchrotron SOLEIL - L'Orme des Merisiers, Saint-Aubin - BP 48 91192 Gif-sur-Yvette cedex, France

<sup>5</sup>Department of Physics, UFR of Sciences and Technologies, University Assane Seck of Ziguinchor, Ziguinchor, Senegal

<sup>6</sup>CEA-DAM-DIF, Bruyères-le-Châtel, F-91297 Arpajon Cedex, France

<sup>7</sup>Department of Physics, Jordan University of Science and Technology, Irbid 22110, Jordan

**Abstract.** Absolute cross sections for the *K*-shell photoionization of boron-like (B-like)  $O^{3+}$  ions were measured by employing the ion-photon merged-beam technique at the SOLEIL synchrotron-radiation facility in Saint-Aubin, France. High-resolution spectroscopy with  $E/\Delta E \approx 5000$  ( $\approx 110$  meV, FWHM) was achieved with photon energy from 540 eV up to 600 eV. Several theoretical approaches, including R-Matrix, Multi-Configuration Dirac-Fock and Screening Constant by Unit Nuclear Charge were used to identify and characterize the strong  $1s \rightarrow 2p$  and the weaker  $1s \rightarrow 3p$  resonances observed in the *K*-shell spectra of this ion. The trend of the integrated oscillator strength and autoionisation width (natural line width) of the strong  $1s \rightarrow 2p$  resonances along the first few ions of the B-like sequence is discussed.

PACS numbers: 32.80.Fb, 31.15.Ar, 32.80.Hd, and 32.70.-n

Short title: *K*-shell photoionization of B-like atomic oxygen ions

Submitted to: *J. Phys. B: At. Mol. Opt. Phys.* : 27 May 2022

§ Corresponding author, E-mail: b.mclaughlin@qub.ac.uk

† Corresponding author, E-mail: jean-marc.bizau@u-psud.fr

## 1. Introduction

Single and multiply ionisation stages of C, N, O, Ne and Fe have been observed in the ionized outflow in the planetary nebulae NGC 4051, measured with the satellite *XMM-Newton* [1] in the soft-x-ray region. Low ionized stages of C, N and O have also been used in the modelling of x-ray emission from OB super-giants [2]. Multiply ionization stages of O and Fe are also seen in the *XMM-Newton* spectra from the Seyfert galaxy NGC 3783, including UV imaging, x-ray and UV light curves, the 0.2 – 10 keV x-ray continuum, the iron *K* - emission line, and high-resolution spectroscopy in the modelling of the soft x-ray warm absorber [3]. Detailed photoionization models of the brightest cluster of star formation in the blue compact dwarf galaxy Mrk 209 required abundances for ions of oxygen and nitrogen [4]. O [IV] *K*-lines are seen in the supernova remnant Cassiopeia (Cas A) in the infrared spectra taken by the Spitzer Space Telescope [5]. In Seyfert galaxies based on photoionization models, O IV comes from higher ionization states and lower density regions and is an accurate indicator of the power of the active galactic nuclei (AGN) [6]. In the present study we focus our attention on obtaining detailed spectra on the triply ionized oxygen ion  $O^{3+}$  (O IV) in the vicinity of its *K* - edge.

Recent wavelength observations of *K*-transitions in atomic oxygen, neon and magnesium and their ions with x-ray absorption lines have been made with the High Energy Transmission Grating (HETG) on board the *CHANDRA* satellite [7]. Strong absorption *K*-shell lines of atomic oxygen, in its various ionized forms, have been observed by the *XMM-Newton* satellite in the interstellar medium, through x-ray spectroscopy of low-mass x-ray binaries [8]. The *CHANDRA* and *XMM - Newton* satellite observations may be used for identifying the absorption features present in astrophysical sources, such as active galactic nuclei and x-ray binaries and for assistance in benchmarking theoretical calculations [9, 10].

Few experiments have been devoted to the study of *K*-shell photoionization on oxygen ions. Auger spectra of singly and doubly core-excited oxygen ions emitted in the collision of fast oxygen-ion beams with gas targets and foils were measured by Bruch and co-workers [11]. *K*-shell x-ray lines from inner-shell excited and ionized ions of oxygen, were observed using the Lawrence Livermore National Laboratory EBIT. With a multi-ion model they were able to identify the observed *K*-shell transitions of oxygen ions from  $O^{2+}$  to  $O^{5+}$ .

Up to now, *K*-shell photoionization cross-section results have been obtained only for  $O^+$  ions by Kawatsura et al [12]. Measurements were made at Spring-8, using the merged-beam technique, on relative cross sections for double photoionization spectra in the energy range of the  $1s \rightarrow 2p$  resonances, using a limited resolving power  $\sim 310$ . *K*-shell single and double photoionization spectra of neutral oxygen have also been obtained [13, 14, 15], recently revisited with high resolution at the Advanced Light Source (ALS) and benchmarked against calculations using the R-matrix with pseudo-states method [16, 17].

Theoretically, resonance energies and line widths for Auger transitions in B-like atomic ions have been calculated using a variety of methods, such as  $1/Z$  perturbation theory [18, 19, 20, 21, 22], multi-configuration Dirac Fock (MCDF) [23, 24], the Saddle-Point-Method (SPM) with R-matrix, complex-coordinate rotation methods [25, 26, 27, 28, 29]. Chen and Craseman [23, 24] calculated Auger and radiative decay of  $1s$  vacancy states in the boron isoelectronic sequence using the Multi-configuration-Dirac-Fock approach (MCDF). Sun and co-workers [30] used the saddle-point method

with rotation to calculate energy levels and Auger decay widths for the  $1s2s^22p^2$  and  $1s2s2p^3\ ^{2,4}L$  levels in B-like carbon and found suitable agreement with the re-calibrated spectrum of Bruch and co-workers [31] and the combined theoretical work and high resolution synchrotron measurements performed at the ALS [32]. In the case of  $O^{3+}$  ions, recent saddle-point with rotation calculations by Sun and co-workers [33] for the energy levels and Auger and radiative decay rates for the  $1s2s^22p^2$  and  $1s2s2p^3\ ^{2,4}L$  levels were compared to the earlier beam-foil experimental measurements of Bruch and co-workers [11], the MCDF work of Chen and Craseman [23, 24] and further extended to the higher lying  $1s2p^4$  levels of other B-like ions [34].

State-of-the-art *ab initio* calculations for Auger inner-shell processes were first performed on this B-like system by Zeng and Yuan [35] and then by Pradhan and co-workers [36] using the R-matrix method [37]. This work followed a similar procedure to *K*-shell studies on Be-like  $B^+$  ions by Petrini [38]. Garcia and co-workers [39], further extended this work by using the R-matrix optical potential method within an intermediate-coupling scheme [40]. Photoionization from the ground state, along the oxygen iso-nuclear sequence was investigated, in the photon energy region of the *K*-edge. In the present study we compare our results from the multi-configuration Dirac Fock (MCDF), R-matrix with pseudo-states (RMPS) approach, and the SCUNC semi-empirical methods [41, 42] with measurements made at SOLEIL, prior EBIT measurements [43], *XMM* and *CHANDRA* satellite observations [3, 44, 45, 8, 7] and other theoretical results [23, 24, 35, 36, 39, 46].

In this paper we present detailed measurements of the absolute *K*-shell single photoionisation cross sections for B-like oxygen ions, in the 542–548 eV region and 594–599 eV photon energy range that were explored experimentally. Theoretical predictions are made from the Screening Constant by Nuclear Unit Charge (SCUNC), MCDF and R-matrix with pseudo-states methods to compare with the measurements. These calculations enable the identification and characterization of the very strong  $1s \rightarrow 2p$  and the weaker  $1s \rightarrow 3p$  resonance peaks observed in the B-like oxygen spectra. The present investigation provides absolute values (experimental and theoretical) for photoionization cross sections for the  $n=2$  inner-shell resonance energies, natural line widths and resonance strengths, occurring for the interaction of a photon with the  $1s^22s^22p\ ^2P^o$  ground state and  $1s^22s2p^2\ ^4P$  metastable state of the  $O^{3+}$  ion. Our work would appear to be the first time that experimental measurements have been performed on this prototype B-like system in the photon energy region of the *K*-edge, and complements our recent studies on *K*-shell photoionization of atomic nitrogen ions [47, 48, 49] and previous investigations on B-like carbon,  $C^+$  [32] at the ALS, in the vicinity of the *K*-edge.

The layout of this paper is as follows. Section 2 briefly outlines the experimental procedure used. Section 3 presents the theoretical work. Section 4 presents a discussion of the results obtained from both experiment and theory. In section 5 we present a discussion of the variation of the integrated oscillator strengths and line widths for the first three ions of the B-like sequence with increasing charge state. Finally in section 6 conclusions are drawn from the present investigation.

## 2. Experiment

### 2.1. Ion production

The present measurements were made using the MAIA (Multi-Analysis Ion Apparatus) set-up, permanently installed on branch A of the PLEIADES beam line [50, 51] at SOLEIL. The set-up and the experimental procedure have been described previously in detail [47]. Here we will only give a brief description of the set-up and procedure. A continuous oxygen ion beam is produced in a permanent magnet Electron Cyclotron Resonance Ion Source (ECRIS) where a micro leak (electrically driven) is used to introduce oxygen gas at continuous rate. A 12.6 GHz radio wave is used to heat the plasma at a power of approximately 40W. The ions are extracted from the plasma by application of a constant 4 kV bias on the source. The ion beam is selected in mass/charge ratio by a dipole magnet before being collimated and merged with the photon beam in the 50 cm long-interaction region. After interaction, the charge state of the ions is analyzed by a second dipole magnet. The parent ions are collected in a Faraday cup, and the photo-ions which have lost an electron (or increase in charge state by one) in the interaction are counted using channel plates.

### 2.2. Excitation source

The photon beam is monochromatised synchrotron radiation from the PLEIADES beam line [50, 51]. In the photon energy range considered here, a permanent-magnet Apple II undulator with 80 mm period is used. The light is monochromatised by a plane-grating monochromator with no entrance slit. The high-flux 600 lines/mm grating was used for this work. High spectral purity is obtained by a combination of a quasi-periodic design for the undulator and the use of a varied groove depth for the plane grating. The photon energy is determined using a double-ionization chamber of the Samson type [52]. For this work, we used the  $1s \rightarrow 4p\sigma$  transition in the  $O_2$  gas [53] and  $3d \rightarrow 6p$  transitions in Xe gas [54] for calibration purposes. The photon energy is corrected for Doppler shift resulting from the velocity of the oxygen ions. We note that during the experiment a misalignment in the monochromator optics did not allow us to reach the optimum resolution and accuracy on the photon energy.

### 2.3. Experimental procedure

The merged-beam set-up allows for the determination of absolute photoionization cross sections. At a given photon energy, the cross sections  $\sigma$  are obtained from,

$$\sigma = \frac{Se^2\eta\nu q}{IJ\epsilon \int_0^L \frac{dz}{\Delta x \Delta y F(z)}}, \quad (1)$$

where  $S$  is the counting rate of photo-ions measured with the channel-plates. A chopper, placed at the exit of the photon beam line, allows to subtract from the photo-ions signal the background produced by collisional-ionization processes, charge stripping on the collimator slits or autoionizing decay of metastable excited states produced in the ECRIS. In (1),  $q$  is the charge state of the target ions,  $\nu$  is the velocity of the ions in the interaction region determined from the potentials applied to the ECRIS and the interaction region (see below) and  $I$  is the current produced by the photons on a AXUV100 IRD photodiode. The efficiency  $\eta$  of the photodiode was calibrated at the Physikalisch-Technische Bundesanstalt (PTB) beam line at BESSY

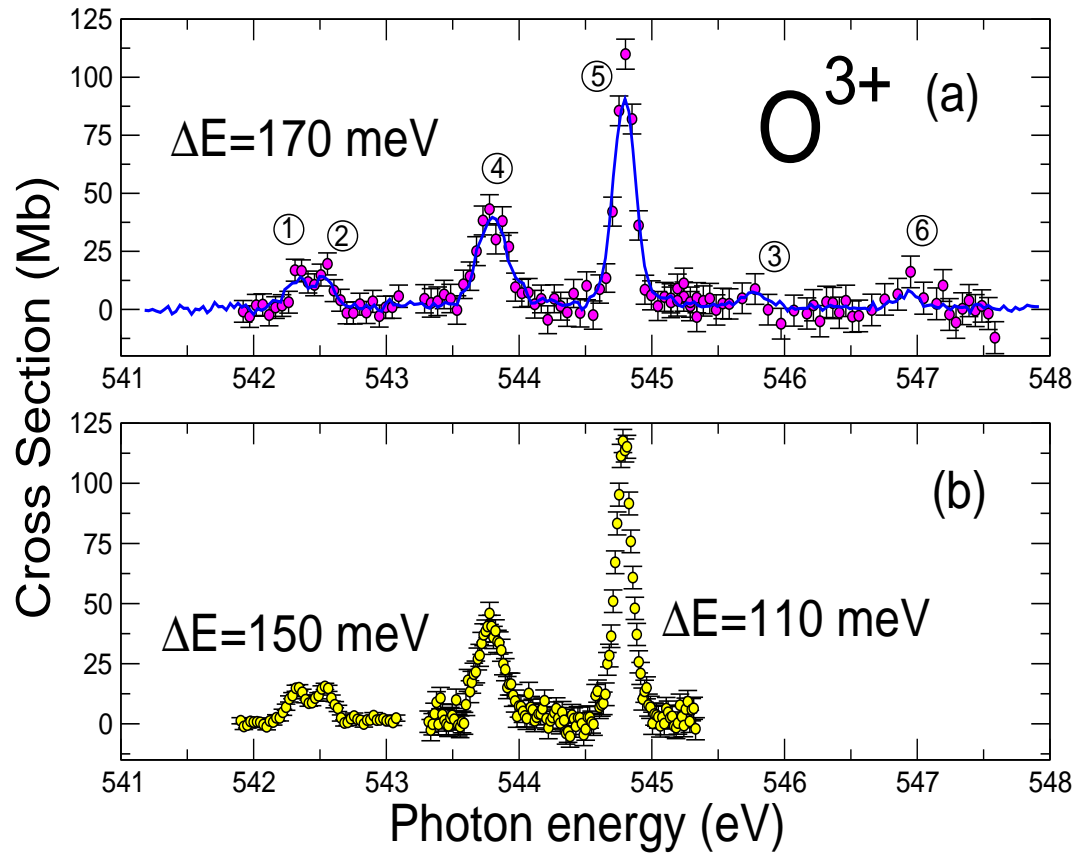


**Figure 1.** (Colour online) SOLEIL experimental  $K$ -shell photoionization cross section of  $O^{3+}$  ions in the 541 - 548 eV photon energy range. Upper panel (a) : Measured with 170 meV band-width. Solid points: the error bars give the total uncertainty; blue line: normalized relative measurements. Lower panel (b) : Lines 1 and 2 measured with 150 meV band-width, only lines 4-5 are measured with the 110 meV band-width. The error bars represent the statistical uncertainty.

**Table 1.** Typical values for the experimental parameters involved in evaluating the absolute cross section measured at a photon energy of 544.8 eV.

$S$	70 Hz
Noise	300 Hz
$\nu$	$4.2 \cdot 10^5 \text{ ms}^{-1}$
Photon flux	$1.3 \cdot 10^{11} \text{ s}^{-1}$
$J$	70 nA
$\epsilon$	0.48
$F_{xy}$	68

in Berlin.  $e$  is the charge of the electron and  $J$  is the current of incident ions measured in the Faraday cup.  $\epsilon$  is the efficiency of the micro-channel plates determined by comparing the counting rate produced by a low intensity ion beam and the current induced by the same beam in the Faraday cup.  $\Delta x \Delta y F(z)$  is an effective beam area ( $z$  is the propagation axis of the two beams), where  $F$  is a two-dimensional form factor determined using three sets of  $xy$  scanners placed at each end and in the middle of the interaction region. The length  $L$  of the interaction region is fixed by applying -1 kV bias on a 50 cm long tube placed in the interaction region, resulting in a different velocity for the photo-ions produced inside and outside the tube. Typical values of the parameters involved in equation 1, measured at a photon energy of 544.8 eV, are given in table 1.

The accuracy of the measured cross sections is determined by statistical fluctuations on the photo-ion and background counting rates and a systematic contribution resulting from the measurement of the different parameters in equation 1. The latter is estimated to be 15% and is dominated by the uncertainty on the determination of the photon flux, the form factor and detector efficiency. To record the single-photoionization spectra, the field in the second dipole magnet is adjusted to detect with the channel plates the photo-ions which have gained one charge while the photon energy is scanned. Two acquisition modes have been used. One with no voltage applied on the interaction tube, allowing better statistics since the whole interaction length of the photon and ion beams is used. In this mode, only relative cross sections are obtained. In the second mode, the voltage is applied to the tube to define the interaction length  $L$ , allowing the determination of cross sections in absolute value.

### 3. Theory

#### 3.1. SCUNC: B-like Oxygen

The starting point of the Screening Constant by Unit Nuclear Charge formalism is the total energy of the  $(N\ell n\ell';^{2S+1}L^\pi)$  excited states of two electron systems given by (in Rydberg units),

$$E(N\ell n\ell';^{2S+1}L^\pi) = -Z^2 \left[ \frac{1}{N^2} + \frac{1}{n^2} [1 - \beta(N\ell n\ell';^{2S+1}L^\pi; Z)]^2 \right]. \quad (2)$$

In this equation, the principal quantum numbers  $N$  and  $n$  are respectively for the inner and the outer electron of the He-like iso-electronic series. The  $\beta$ -parameters are screening constants by unit nuclear charge expanded in inverse powers of  $Z$  and are

given by the expression,

$$\beta(N\ell n\ell'; {}^{2S+1}L^\pi) = \sum_{k=1} f_k \left(\frac{1}{Z}\right)^k \quad (3)$$

where  $f_k(N\ell n\ell'; {}^{2S+1}L^\pi)$  are parameters that are evaluated empirically from existing experimental measurements on resonance energies. In the same way one may get the Auger widths  $\Gamma$  in Rydbergs (1 Rydberg = 13.60569 eV) from the formula

$$\Gamma(\text{Ry}) = Z^2 \left[ 1 - \sum_q f_q \left(\frac{1}{Z}\right)^q \right]^2. \quad (4)$$

For the B-like  $O^{3+}$  ion the total energies of the  $1sN s^x n p^y {}^{2S+1}L$  states are given by

$$\begin{aligned} E(1sN s^x n p^y; {}^{2S+1}L^\pi) = & -Z^2 \left[ 1 + \frac{x}{N^2} \left( 1 - \sum_{k=1} f_k \left(\frac{1}{Z}\right)^k \right)^2 \right] \\ & - Z^2 \left[ \frac{y}{n^2} \left( 1 - \sum_{k=1} f'_k \left(\frac{1}{Z}\right)^k \right)^2 \right]. \end{aligned} \quad (5)$$

Here  $x$  and  $y$  are the number of electrons in the  $s$  and  $p$  orbitals respectively. As the  $\ell$ -orbital quantum number is equal to zero in the  $N s^x$  orbital, we neglect the dependence of the  $\beta$ -parameters on  $\ell$ . This approximation permits one to simplify equation (3) for each of the  $1sN s^x n p^y {}^{2S+1}L^\pi$  resonances where only one parameter (here  $f_1$ ) is to be evaluated empirically and similarly  $f_2$  for the Auger widths.

The Advanced Light Source experimental measurements of Schlachter and co-workers on K-shell photoionization of B-like carbon ions [32] were used to determine the appropriate empirical parameters  $f_k$  and  $f_q$  for the resonance energy and Auger widths. The ALS experimental data of Schlachter and co-workers on  $C^+$  ( $Z = 6$ ) [32] for the  $1s2s^22p^2 {}^2D$ ,  $1s2s^22p^2 {}^2P$ , and  $1s2s^22p^2 {}^2S$  levels are located at  $287.93 \pm 0.03$ ,  $288.40 \pm 0.03$  and  $289.90 \pm 0.03$ , respectively, where the values are given in eV. Using the ground state energy of  $C^+$ ,  $-1018.8467$  eV [55] we obtain  $f_1({}^2D) = 1.7903 \pm 0.0003$ ,  $f_1({}^2P) = 1.7944 \pm 0.0003$  and  $f_1({}^2S) = 1.8075 \pm 0.0003$  for use in equation (2). The ALS experimental values for the Auger widths (given in meV) on  $C^+$  for these same resonances, are respectively  $105 \pm 15$ ,  $59 \pm 6$ , and  $112 \pm 25$  and we find that  $f_2({}^2D) = 5.9121 \pm 0.0060$ ,  $f_2({}^2P) = 5.9341 \pm 0.0033$  and  $f_2({}^2S) = 5.9093 \pm 0.0096$  which are used in equation (4). The SCUNC estimates for the resonance energies and Auger widths for  $O^{3+}$  and  $N^{2+}$  using these values are given in Tables 2 – 5.

### 3.2. MCDF: B-like Oxygen

Multi-configuration Dirac-Fock (MCDF) calculations were performed based on a full intermediate coupling regime in a  $jj$ -basis using the code developed by Bruneau [56]. Photoexcitation cross sections have been carried out for B-like atomic oxygen ions in the region of the K-edge. Only electric dipole transitions have been computed using length and velocity forms. In the present study, oscillator strengths calculated using the two gauges differ by less than 8%. Photoexcitation from the two levels ( ${}^2P_{1/2,3/2}^o$ ) of the ground configuration  $1s^22s^22p$  and from metastable levels ( ${}^4P_{1/2,3/2,5/2}$ ) of the

configuration  $1s^2 2s 2p^2$  have been calculated separately. In both cases, multiple orbitals with the same quantum number have been used in order to describe the correlation and relaxation effects. Wavefunctions have been calculated minimizing the Slater transition state. Each electric dipole transition has been dressed by a Lorentzian profile with a full width half maximum (FWHM) equal to 10 meV.

Calculations of the  ${}^2P_{1/2,3/2}^o$  photoexcitation cross sections have been performed using the following set of configurations. The initial configurations used were :  $\underline{1s^2 2s^2 np}$  (with  $n=2, \dots, 5$ ),  $\underline{1s^2 2s 2p ns}$  (with  $n=3, \dots, 5$ ). The final configurations were :  $1s 2s^2 2p^2$ ,  $1s 2s^2 2p np$  (with  $n=3, \dots, 5$ ). Such notation means that the radial functions  $1s_{1/2}$  and  $2p_{1/2,3/2}$  are not the same for initial and final configurations. Similarly for the  ${}^4P_{1/2,3/2,5/2}$  levels, photoexcitation cross sections have been performed using the following set of configurations : initial configurations :  $1s^2 2s 2p np$  (with  $n=2, \dots, 4$ ),  $1s^2 2s 3\ell^2$  ( $\ell=0, 1, 2$ ),  $1s^2 2s 4\ell^2$  ( $\ell=0, 1, 2$ ),  $1s^2 2s 3p 4p$ , final configurations :  $1s 2s np n' p n'' p$  (with  $n, n'$  and  $n''=2, \dots, 4$ ).

The wavefunctions have been calculated minimizing the following energy functional,

$$E = \frac{\sum_{\alpha} (2J_{\alpha} + 1) E_{\alpha}}{2 \sum_{\alpha} (2J_{\alpha} + 1)} + \frac{\sum_{\beta} (2J_{\beta} + 1) E_{\beta}}{2 \sum_{\beta} (2J_{\beta} + 1)} \quad (6)$$

where  $\alpha$  and  $\beta$  run over all the initial and final states, respectively.

### 3.3. R-matrix: B-like Oxygen

The  $R$ -matrix method [40], with an efficient parallel implementation of the codes [57, 58, 59] was used to determine all the cross sections presented here, for both the initial  ${}^2P^o$  ground state and the  ${}^4P$  metastable states. Cross section calculations were carried out in  $LS$ -coupling with 390-levels retained in the close-coupling expansion. The Hartree-Fock  $1s$ ,  $2s$  and  $2p$  tabulated orbitals of Clementi and Roetti [60] were used with  $n=3$  physical and  $n=4$  pseudo orbitals of the  $O^{3+}$  ion determined by energy optimization on the appropriate physical and hole-shell states [61], using the atomic structure code CIV3 [62]. The  $n=4$  pseudo-orbitals are included to account for core relaxation and additional correlation effects in the multi-configuration interaction wavefunctions. All the  $O^{4+}$  residual ion states were then represented by using multi-reference-configuration-interaction (MRCI) wave functions. The non-relativistic  $R$ -matrix approach was used to calculate the energies of the  $O^{3+}$  bound states and the subsequent PI cross sections. PI cross sections out of the  $1s^2 2s 2p$   ${}^2P^o$  ground state and the  $1s^2 2s 2p^2$   ${}^4P$  metastable state were then obtained for all total angular momentum scattering symmetries that contribute.

The  $R$ -matrix with pseudo-states method (RMPS) was used to determine all the cross sections (in  $LS$  - coupling) with 390 levels of the  $O^{4+}$  residual ion included in the close-coupling calculations. Due to the presence of metastable states in the beam, PI cross-section calculations were performed for both the  $1s^2 2s 2p$   ${}^2P^o$  ground state and the  $1s^2 2s 2p^2$   ${}^4P$  meta stable state of the  $O^{3+}$  ion.

The scattering wavefunctions were generated by allowing three-electron promotions out of selected base configurations of  $O^{3+}$  into the orbital set employed. Scattering calculations were performed with twenty continuum functions and a boundary radius of 9.4 Bohr radii. For both the  ${}^2P^o$  ground state and the  ${}^4P$  metastable states the outer region electron-ion collision problem was solved (in the resonance region below and between all the thresholds) using a suitably chosen fine



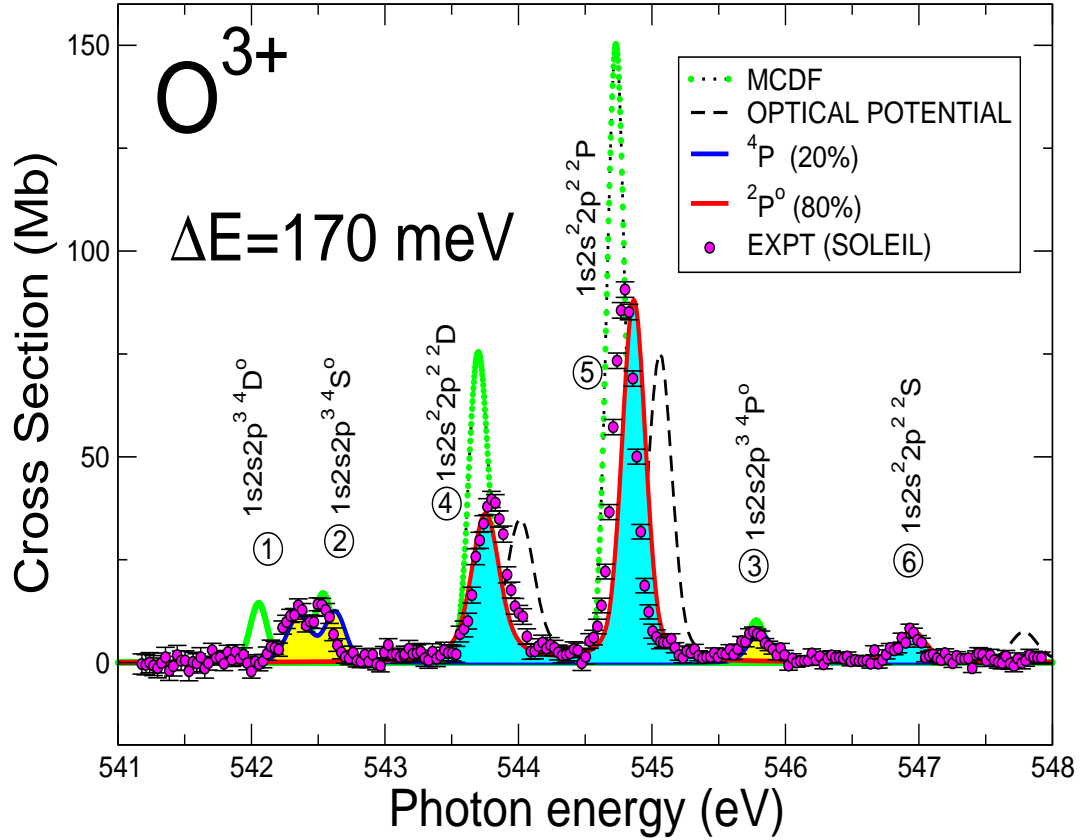


**Figure 2.** (Colour online) Photoionization cross sections for  $O^{3+}$  ions measured with a 170 meV band pass in the region of  $1s \rightarrow 2p$  photo-excitations. Solid points (magenta), experimental cross sections. The error bars give the statistical uncertainty of the experimental data. The R-matrix (RMPS, solid red line, ground state, 80%  $2P^o$ , metastable, blue line 20%  $4P$ ). Dotted line with solid green circles are the present MCDF calculations (80%  $2P^o$  and 20%  $4P$ ). The optical potential R-matrix results (dashed black line 80%  $2P^o$ ) are from the results of Garcia and co-workers [39]. Theoretical work shown was convoluted with a Gaussian profile of 170 meV FWHM and a weighting of the ground and metastable states (see text for details) to simulate the measurements. Tables 2 and 3 gives the designation of the resonances ① - ⑥ in this photon energy region.

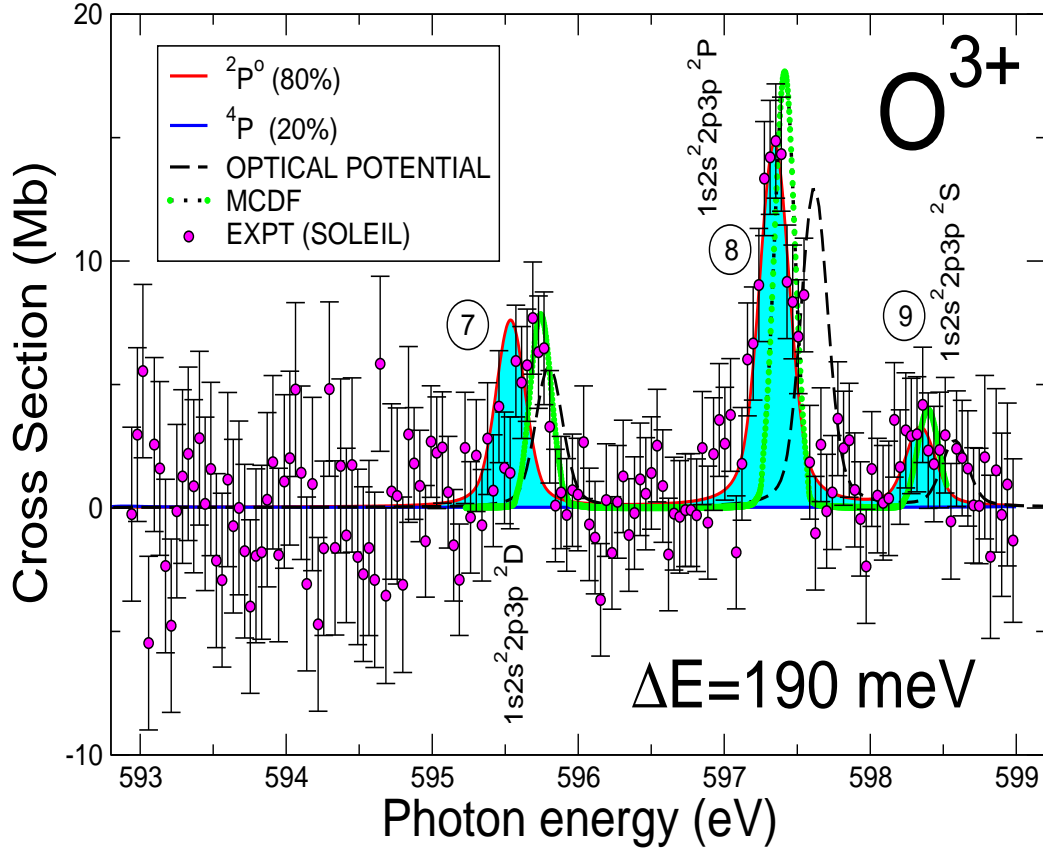


**Figure 3.** (Colour online) Photoionization cross sections for  $O^{3+}$  ions measured with a 190 meV band pass in the region of the  $1s \rightarrow 3p$ . Solid circles : Experimental cross section measured in the relative mode, normalized on the R-matrix results (see text). The error bars give the statistical uncertainty of the experimental data. R-matrix (RMPS, red line 80%  $^2P^o$ , blue line 20%  $^4P$ ). MCDF calculations (dotted black line with green circles 80%  $^2P^o$ ). The optical potential (dashed black line 80%  $^2P^o$ ) R-matrix results of Garcia and co-workers [39]. Theoretical work shown was convoluted with a Gaussian profile of 190 meV FWHM and a weighting of the ground and metastable states (see text for details) to simulate the measurements. Table 4 gives the designation of the resonances ⑦ - ⑨ in this photon energy region.

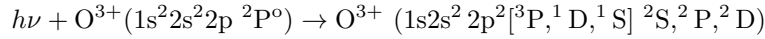
energy mesh of  $2 \times 10^{-7}$  Rydbergs ( $\approx 2.72 \mu\text{eV}$ ) to fully resolve all the resonance structure in the PI cross sections. Radiation and Auger damping were also included in the cross section calculations.

#### 4. Results and Discussion

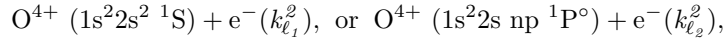
Figure 1 displays the photoionization cross sections measured at SOLEIL in the region of the  $1s \rightarrow 2p$  resonances. In the upper panel, the continuous line shows the cross section measured in the relative mode with  $170 \pm 4$  meV band-width (BW), and the open points are the ones obtained with a larger step in the absolute mode. The error bars give the total accuracy of the cross sections. The lower panel shows the cross sections recorded in the relative mode with improved resolution,  $150 \pm 25$  meV BW for the region 542-543 eV, and  $110 \pm 13$  meV for the region 543.3-545.3 eV. The relative measurements have been placed on an absolute scale by normalization to the absolute cross section by means of the area under the lines, which is independent of the experimental BW. The error bars on the relative measurements give the statistical uncertainty.

$K$ -shell photoionization contributes to the ionization balance in a more complicated way than outer-shell photoionization. In fact  $K$ -shell photoionization when followed by Auger decay couples three or more ionization stages instead of two in the usual equations of ionization equilibrium [63]. Promotion of a  $K$ -shell electron in  $O^{3+}$  ions to an outer  $np$ -valence shell ( $1s \rightarrow np$  transition) from the ground state produces states that can autoionise, forming an  $O^{4+}$  ion and an outgoing free electron.

The  $1s \rightarrow 2p$  photo-excitation process on the  $1s^2 2s^2 2p^2 P^o$  ground-state of B-like oxygen ion is,



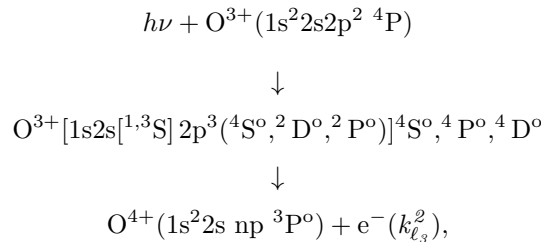
which can decay via autoionisation mainly to



where  $k_{\ell_i}^2$  ( $i = 1, 2$ ) represent the energies of the outgoing Auger electrons from the two different decay processes, respectively.

Three Auger lines are expected in the spectrum, corresponding to the  $1s 2s^2 2p^2 ^2S$ ,  $^2P$  and  $^2D$  resonances, due to  $1s \rightarrow 2p$  core-excited states from the ground state of the parent ion. In the present experimental investigations,  $O^{3+}$  ions are extracted from a high temperature plasma inside the ECRIS, where the ions are produced in all the excited states, and in particular the  $1s^2 2s 2p^2 ^4P$  metastable state has a lifetime long enough to travel to the interaction region and contribute to the photoionization signal.

For the  $1s^2 2s 2p^2 ^4P$  metastable state, autoionisation processes occurring by the  $1s \rightarrow 2p$  photo-excitation process are;



giving rise to three additional lines, which are observed in the spectra as illustrated in Figures 1 and 2, where  $k_{\ell_3}^2$  represent the energy of the outgoing Auger electron.

Figure 2 compares the experimental cross sections obtained with a 170 meV BW (continuous line on the top panel of Figure 1) with our theoretical MCDF and R-matrix results for the photon energy range of 541–548 eV. The R-matrix optical potential calculations (dashed line) are included for completeness. The error bars on the experimental data give the statistical uncertainty. Since the relative population of  $^4P$  metastable term of the  $O^{3+}$  ion present in the parent experimental beam cannot be determined experimentally, theory may be used to estimate its content. From our theoretical R-matrix studies on this system we find that an admixture of 80 % ground states and 20 % metastable states in the parent ion beam appears to give the closest agreement between theory and experiment. The same relative populations have been found in previous experimental studies on B-like ions :  $C^+$  [32] and  $N^{2+}$  [49], performed with the same type of ion source.

The peaks found in the theoretical photoionization cross sections spectrum were fitted to Fano profiles for overlapping resonances [64, 65, 66] as opposed to the energy derivative of the eigenphase sum method [67, 68, 69]. The theoretical values for the natural line widths  $\Gamma$  determined from this procedure are presented in Tables 2 and 3 for the strong peaks in the photon region 540 eV to 549 eV and compared with results obtained from the high-resolution SOLEIL synchrotron measurements and with other methods. Note, in Table 3 we have included the beam-foil values quoted by Sun *et al* [33] who reinterpreted the measurements of Bruch and co-workers [11].

We note the good agreement obtained by both theoretical results for the position and intensity of the lines. The R-matrix calculations include Auger and radiation damping, missing from the MCDF calculations and give lines positions and intensities in closer agreement with experiment. Tables 2 and 3 summarizes our experimental, R-matrix and MCDF values for the position, width and strength of the observed lines, as well as the results of our SCUNC calculations with previously published experimental [11, 43] and theoretical data [35, 36, 39]. Our experimental values, including experimental band-widths, were obtained by fitting the data with Voigt profiles to the spectra shown on Figure 1.

Concerning the excitation energy of the lines, the EBIT measurements [43] give values significantly lower (by 0.5 eV) than our values. We note that, in the EBIT work, only the lines due to the ions in the ground states were observed, with an insufficient resolving power ( $\sim 1100$ ) to separate the individual lines. A comparison of the various theoretical predictions shows that our R-matrix with pseudo-states (RMPS) calculations give the best overall agreement with experiment, almost all energies lying within the experimental uncertainties. Our semi-empirical SCUNC calculations give satisfactory agreement with experiment, with a maximum discrepancy of 0.3 eV. Considering the work of Garcia *et al* [39], we remark that better agreement is achieved from simple SUPERSTRUCTURE calculations (approximation AS1 in paper [39]) rather than by their more sophisticated R-matrix calculations.

As in the case for neutral oxygen [16, 17, 10] there is a discrepancy in the position of the strongest  $1s \rightarrow 2p$  transition in the  $K$ -shell spectrum of  $O^{3+}$  ( $O\ IV$ ) compared with very recent *Chandra* HETG observations [7] (where the  $K_\alpha$  lines from two elements are observed at 22.6969 Å, 546.260 eV and 22.6965 Å, 546.270 eV). In contrast to this the present high resolution measurements made at SOLEIL (22.758 Å, 544.794 eV), shows excellent agreement with previous *XMM* observations (22.7769  $\pm$  0.02 Å, 544.340 eV and 22.75  $\pm$  0.02 Å, 544.985 eV) [3, 8], *Chandra* observations (22.74  $\pm$  0.02 Å, 545.225 eV and 22.7509  $\pm$  0.02 Å, 544.946 eV) [44, 45] and EBIT measurements (22.741  $\pm$  0.005 Å, 545.201 eV) [43] including the current R-matrix

with pseudo-states (RMPS) predictions (22.7586 Å, 544.869 eV).

Our measured widths are in agreement with theoretical predictions for the  $4S^o$ ,  $2D$  and  $4P^o$  lines, but are systematically lower compared to theory for the  $2P$  and  $2S$  lines. All the theoretical strengths in Tables 2 and 3 have been weighted by the 80 % and 20 % population of the ground and metastable states, respectively.

Figure 3 illustrates the cross sections for the photon energy range 593–599 eV, in the vicinity of the  $1s \rightarrow 3p$  transitions, which occurs from the ground state of the  $O^{3+}$  ion. The measurements in this energy region were taken in the relative mode with a spectral resolution of  $190 \pm 20$  meV. They are compared to the results of our R-matrix RMPS, MCDF and the R-matrix Optical [39] calculations. The relative measurements have been normalized on the area of resonance line 8 calculated with the R-matrix parallel suite of codes. As previously, to compare directly with experiment all the theoretical calculations were convoluted with a Gaussian function of 190 meV FWHM and weighted 80% for the ground-state population and 20% for the metastable state. In this energy region it is seen that the metastable contribution is negligible. Our experimental and theoretical excitation energies, widths and strengths are given in Table 4. Due to limited statistics, the natural width could only be obtained experimentally for the most intense  $1s \rightarrow 3p$  transitions, where the strongest peak observed in this photon energy region is due to the  $1s^2 2s^2 2p \ ^2P^o \rightarrow 1s 2s^2 2p 3p \ ^2P$  transition. We find an experimental value for the energy of this resonance to be located at  $597.348 \pm 0.123$  eV. Theoretical predictions from the R-matrix with pseudo-states method (RMPS) give a value of 597.345 eV for the energy of this resonance and the MCDF value is 597.419 eV. For this  $1s \rightarrow 3p$  resonance the SOLEIL experimental measurements yield a value  $133 \pm 71$  meV for the Auger width compared to the R-matrix with pseudo-states method (RMPS) of 122 meV. SCUNC estimates give for this  $1s \rightarrow 3p$  resonance peak an energy position of 597.629 eV and an Auger width of 37 meV. The R-matrix with pseudo-states method (RMPS) calculations give excitation energies in excellent agreement with measurements, while the predictions for this same  $1s \rightarrow 3p$  resonance line from the MCDF and SCUNC methods indicate the energy is at a higher energy, respectively 0.06 eV and 0.3 eV.

In tables 2 and 3 we have used the Heisenberg uncertainty principle ( $\Delta E \Delta t = \hbar/2$ , i.e.  $\Gamma = 658.21189/2\tau$ , where the natural line width  $\Gamma$  is in meV and  $\tau$  the lifetime, is in femto-seconds) to convert the MCDF and Saddle point Auger rates [23, 24, 33] for the  $1s \rightarrow 2p$  resonance transitions to widths (in meV) for comparison purposes.

## 5. Auger widths and $f$ -values for B-like ions; $C^+$ , $N^{2+}$ and $O^{3+}$ ions

To gain some physical insight into how a photon interacts with ions along the B-like sequence, we draw comparison with previous and more recent experimental and theoretical work on the B-like ions;  $C^+$  [32],  $N^{2+}$  [49],  $O^{3+}$  [33] and the current investigation on  $O^{3+}$  in the  $K$ -shell region. Results for the cross sections and resonance parameters from the R-matrix with pseudo-states (RMPS) approximation provide accurate results which are used here for comparison purposes across all three ions. In order to have a consistent comparison with the earlier ALS experimental data made on B-like carbon ion,  $C^+$  [32], RMPS calculations were performed on the  $C^+$  B-like ion using the same 390-level approximation presently used for  $O^{3+}$  and previously for  $N^{2+}$  [49] ions. Resonance parameters were extracted and a consistent comparison made between the experimental and theoretical work for all three ions of the B-like sequence, not available currently with other theoretical approaches.

**Table 2.** B-like atomic oxygen ions, quartet core-excited states. Comparison of the present experimental and theoretical results for the resonance energies  $E_{\text{ph}}^{(\text{res})}$  (in eV), natural line widths  $\Gamma$  (in meV) and resonance strengths  $\bar{\sigma}^{\text{PI}}$  (in Mb eV), for the dominant core photo-excited n=2 states of the  $O^{3+}$  ion, in the photon energy region 541 eV to 548 eV with previous investigations. The experimental error in the calibrated photon energy is estimated to be  $\pm 70$  meV.

Resonance (Label)		SOLEIL (Experiment <sup>†</sup> )	R-matrix (Theory)	MCDF/Others (Theory)
1s2s[ <sup>3</sup> S]2p <sup>3</sup> [ <sup>2</sup> D <sup>o</sup> ] 4D <sup>o</sup> ①	$E_{\text{ph}}^{(\text{res})}$	542.330 $\pm$ 0.082 <sup>†</sup> $\pm$ 0.013 <sup>*</sup>	542.351 <sup>a</sup>	542.058 <sup>b</sup>
		542.933 $\pm$ 0.12 <sup>‡</sup>	542.719 <sup>d</sup>	543.686 <sup>c</sup> 542.552 <sup>e</sup> 542.909 <sup>f</sup>
	$\Gamma$	24 $\pm$ 14 <sup>†</sup>	73 <sup>a</sup> 80 <sup>d</sup>	38 <sup>c</sup> 96 <sup>e</sup> 74 <sup>f</sup>
	$\bar{\sigma}^{\text{PI}}$	2.49 $\pm$ 0.90 <sup>†</sup>	2.59 <sup>a</sup>	2.54 <sup>b</sup>
1s2s[ <sup>1</sup> S]2p <sup>3</sup> [ <sup>4</sup> S <sup>o</sup> ] 4S <sup>o</sup> ②	$E_{\text{ph}}^{(\text{res})}$	542.532 $\pm$ 0.080 <sup>†</sup> $\pm$ 0.011 <sup>*</sup>	542.628 <sup>a</sup>	542.506 <sup>b</sup>
			543.203 <sup>d</sup>	542.557 <sup>c</sup> 542.209 <sup>e</sup> 543.028 <sup>f</sup>
	$\Gamma$	23 $\pm$ 14 <sup>†</sup>	20 <sup>a</sup> 19 <sup>d</sup>	13 <sup>c</sup> 30 <sup>e</sup> 20 <sup>f</sup>
	$\bar{\sigma}^{\text{PI}}$	2.61 $\pm$ 0.99 <sup>†</sup>	2.57 <sup>a</sup>	3.07 <sup>b</sup>
1s2s[ <sup>3</sup> S]2p <sup>3</sup> [ <sup>2</sup> P <sup>o</sup> ] 4P <sup>o</sup> ③	$E_{\text{ph}}^{(\text{res})}$	545.730 $\pm$ 0.079 <sup>†</sup> $\pm$ 0.010 <sup>*</sup>	545.808 <sup>a</sup>	545.773 <sup>b</sup>
			546.131 <sup>d</sup>	547.006 <sup>c</sup> 545.764 <sup>e</sup> 546.692 <sup>f</sup>
	$\Gamma$	70 $\pm$ 23 <sup>†</sup>	59 <sup>a</sup> 60 <sup>d</sup>	29 <sup>c</sup> 76 <sup>e</sup> 55 <sup>f</sup>
	$\bar{\sigma}^{\text{PI}}$	1.44 $\pm$ 1.10 <sup>†</sup>	1.67 <sup>a</sup>	1.82 <sup>b</sup>

<sup>†</sup>SOLEIL, experimental work, \*uncertainty relative to resonance line 5.

<sup>‡</sup>EBIT, experimental work [43].

<sup>a</sup>R-matrix, RMPS present work.

<sup>b</sup>MCDF, present work.

<sup>c</sup>MCDF, Chen and co-workers. [23, 24].

<sup>d</sup>R-matrix, [35].

<sup>e</sup>SCUNC, present work.

<sup>f</sup>Saddle point + complex rotation, [33].

**Table 3.** B-like atomic oxygen ions, doublet core-excited states arising from the configuration  $1s2s^22p^2$ . Comparison of the present experimental and theoretical results for the resonance energies  $E_{\text{ph}}^{(\text{res})}$  (in eV), natural line widths  $\Gamma$  (in meV) and resonance strengths  $\bar{\sigma}^{\text{PI}}$  (in Mb eV), for the dominant core photo-excited  $n=2$  states of the  $O^{3+}$  ion, in the photon energy region 541 eV to 547 eV with previous investigations. The experimental error in the calibrated photon energy is estimated to be  $\pm 70$  meV.

Resonance (Label)		SOLEIL (Experiment <sup>†</sup> )	R-matrix (Theory)	MCDF/Others (Theory)
④ $1s2s^22p^2 [^1D]^2D$	$E_{\text{ph}}^{(\text{res})}$	$543.801 \pm 0.073^{\dagger}$	$543.757^a$	$543.691^b$
		$\pm 0.004^*$	$544.021^d$	$545.539^c$
		$544.614 \pm 1.00^{\parallel}$	$545.465^e$	$543.809^g$
			$544.003^f$	$544.334^j$
	$\Gamma$	$144 \pm 8^{\dagger}$	$131^a$	
			$140^d$	$64^c$
			$27^e$	$151^g$
			$76^f$	$155^j$
	$\bar{\sigma}^{\text{PI}}$	$12.41 \pm 2.59^{\dagger}$	$11.85^a$	$15.32^b$
⑤ $1s2s^22p^2 [^3P]^2P$	$E_{\text{ph}}^{(\text{res})}$	$544.794 \pm 0.071^{\dagger}$	$544.869^a$	$544.731^b$
		$\pm 0.000^*$		
		$545.201 \pm 0.096^{\ddagger}$	$545.299^d$	$545.068^c$
		$544.340 \pm 0.40^+$	$546.909^e$	$544.501^g$
		$544.330 \pm 0.40^+$	$545.066^f$	$544.945^h$
		$545.225 \pm 0.40^{\S}$		$544.985^i$
	$544.946 \pm 0.40^{\S}$		$545.379^j$	
		$545.409 \pm 1.00^{\parallel}$		
	$\Gamma$	$35 \pm 4^{\dagger}$	$75^a$	
			$67^d$	$28^c$
			$14^e$	$78^g$
			$76^f$	$92^j$
	$\bar{\sigma}^{\text{PI}}$	$19.68 \pm 2.59^{\dagger}$	$17.45^a$	$27.90^b$
⑥ $1s2s^22p^2 [^1S]^2S$	$E_{\text{ph}}^{(\text{res})}$	$546.908 \pm 0.085^{\dagger}$	$546.954^a$	$548.783^b$
		$\pm 0.016^*$		
		$547.914 \pm 1.00^{\parallel}$	$547.276^d$	$547.066^c$
			$552.022^e$	$546.711^g$
			$547.791^f$	$547.624^j$
	$\Gamma$	$26 \pm 22^{\dagger}$	$130^a$	
			$125^d$	$58^c$
			$22^e$	$162^g$
			$127^f$	$91^j$
	$\bar{\sigma}^{\text{PI}}$	$3.73 \pm 1.67^{\dagger}$	$1.87^a$	$3.05^b$

<sup>†</sup>SOLEIL, experimental work, \*uncertainty relative to resonance line 5.

<sup>‡</sup>EBIT, experimental work [43].

<sup>||</sup>BEAM-FOIL, experimental work, assignments are from Sun and co-workers [33].

<sup>+</sup>XMM, [3, 8] and <sup>§</sup>CHANDRA observations, [44, 45].

<sup>a</sup>R-matrix, RMPS present work

<sup>b</sup>MCDF, present work, <sup>c</sup>Chen and co-workers. [23, 24].

<sup>d</sup>R-matrix, [35], <sup>e</sup>R-matrix, [36], <sup>f</sup>R-matrix, optical potential [39].

<sup>g</sup>SCUNC, present work.

<sup>h</sup>Flexible Atomic Code (FAC), [46].

<sup>i</sup>HFR, Garcia and co-workers, [39].

<sup>j</sup>Saddle-point + complex rotation, [33].

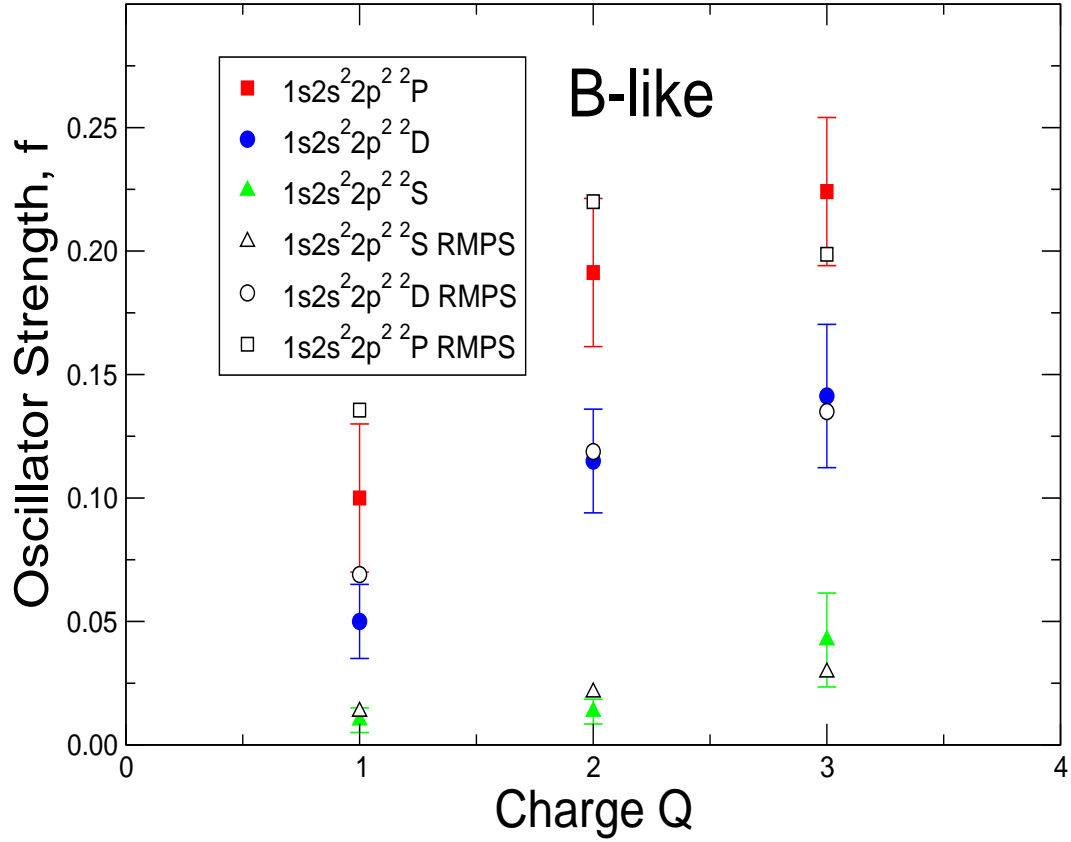


**Figure 4.** (Colour online) Oscillator strengths  $f$  for the  $1s2s^2 2p^2 \ ^2P, \ ^2D, \ ^2S$  Auger states of the first three ions in the B-like sequence versus increasing charge  $Q$ . The Auger states,  $1s2s^2 2p^2 \ ^2S$  (green solid triangles),  $1s2s^2 2p^2 \ ^2D$  (blue solid circles),  $1s2s^2 2p^2 \ ^2P$  (red solid squares), are from experimental studies on  $C^+$  [32],  $N^{2+}$  [49] and the present  $O^{3+}$  investigation. Theoretical results, R - matrix with pseudo-states (RMPS, open triangles  $1s2s^2 2p^2 \ ^2S$ , open squares  $1s2s^2 2p^2 \ ^2P$ , open circles  $1s2s^2 2p^2 \ ^2D$ ), see table 5 for numerical values.



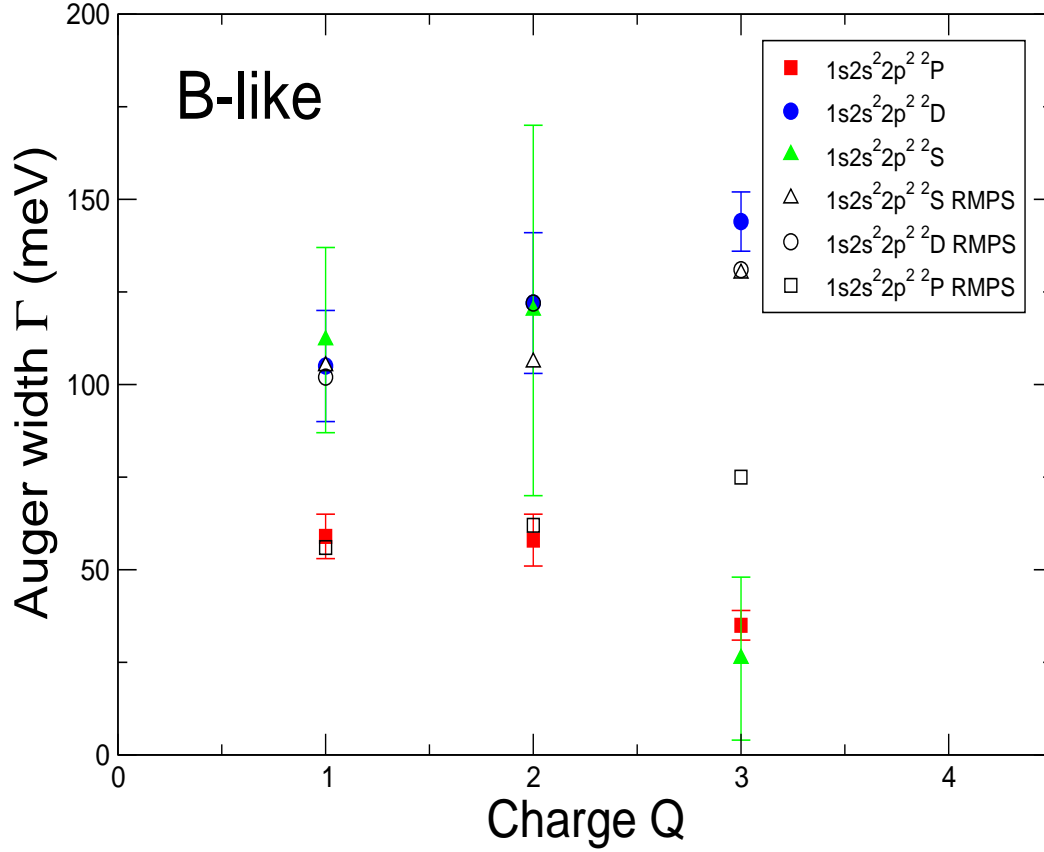


**Figure 5.** (Colour online) Autoionization resonance widths  $\Gamma$  (meV) for the  $1s2s^2 2p^2 \ ^2P, ^2D, ^2S$  Auger states of the first three ions in the B-like sequence versus increasing charge  $Q$ . The Auger states,  $1s2s^2 2p^2 \ ^2S$  (green solid triangles),  $1s2s^2 2p^2 \ ^2D$  (blue solid circles),  $1s2s^2 2p^2 \ ^2P$  (red solid squares), are from experimental studies on  $C^+$ [32],  $N^{2+}$  [49] and the present  $O^{3+}$  investigation. Theoretical results, R - matrix with pseudo-states (RMPS, open triangles  $1s2s^2 2p^2 \ ^2S$ , open squares  $1s2s^2 2p^2 \ ^2P$ , open circles  $1s2s^2 2p^2 \ ^2D$ ), see table 5 for numerical values.

**Table 4.** B-like atomic oxygen ions, doublet core-excited states arising from the configuration  $1s2s^22p3p$ . Comparison of the present experimental and theoretical results for the resonance energies  $E_{\text{ph}}^{(\text{res})}$  (in eV), natural line widths  $\Gamma$  (in meV) for these photo-excited states of the  $O^{3+}$  ion, in the photon energy region 594 eV to 599 eV with previous investigations. The experimental error in the calibrated photon energy is estimated to be  $\pm 110$  meV.

Resonance (Label)		SOLEIL (Experiment <sup>†</sup> )	R-matrix (Theory)	MCDF/Others (Theory)
⑦ $1s2s^22p3p\ ^2D$	$E_{\text{ph}}^{(\text{res})}$	$595.671 \pm 0.134^\dagger$	$595.534^a$ $595.806^c$	$595.749^b$ $595.977^d$
	$\Gamma$	–	$90^a$ $66^c$	$91^d$
⑧ $1s2s^22p3p\ ^2P$	$E_{\text{ph}}^{(\text{res})}$	$597.348 \pm 0.123^\dagger$	$597.352^a$ $597.616^c$	$597.419^b$ $597.629^d$
	$\Gamma$	$133 \pm 71^\dagger$	$122^a$ $75^c$	$37^d$
⑨ $1s2s^22p3p\ ^2S$	$E_{\text{ph}}^{(\text{res})}$	$598.362 \pm 0.175^\dagger$	$598.347^a$ $598.585^c$	$598.382^b$ $598.309^d$
	$\Gamma$	–	$98^a$ $87^c$	$100^d$

<sup>†</sup>SOLEIL, experimental work.

<sup>a</sup>R-matrix, RMPS present work.

<sup>b</sup>MCDF, present work.

<sup>c</sup>R-matrix, optical potential [39].

<sup>d</sup>SCUNC, present work.

The indirect photoionization cross section for each resonance can be derived from the calculated oscillator strengths, where the integrated oscillator strengths  $f$  of the spectra, may be calculated using,

$$\begin{aligned} \sigma(E) &= 2\pi^2 \alpha a_0^2 R_\infty \frac{df}{dE} \\ &= 1.097618 \times 10^{-16} \frac{df}{dE} \text{ eV cm}^2 \end{aligned} \quad (7)$$

where  $\alpha$  is the fine structure constant,  $a_0$  is the Bohr radius,  $R_\infty$  is the Rydberg constant and  $df/dE$  is the differential oscillator strength per unit energy [70, 64]. Rearranging and integrating we have the expression for the oscillator strength  $f$

**Table 5.** B-like ions, doublet core-excited states arising from the configuration  $1s2s^22p^2$ . Comparison of the present experimental and theoretical results for the integrated oscillator strengths  $f$  and the natural line widths  $\Gamma$  (in meV) for the dominant core photo-excited  $n=2$  states of the first three B-like ions with previous investigations.

Resonance (Label)		SOLEIL/ALS (Experiment)	R-matrix (Theory)	Others (Theory)
$1s2s^22p^2 [^1D]^2D$				
C <sup>+</sup>	$f$	$0.05 \pm 0.015^{\ddagger}$	$0.069^a$	
	$\Gamma$	$105 \pm 15^{\ddagger}$	$102^a$ $103^b$	
N <sup>2+</sup>	$f$	$0.115 \pm 0.02^{\dagger}$	$0.119^a$	
	$\Gamma$	$122 \pm 19^{\dagger}$	$122^a$ $109^e$	$123^f$
O <sup>3+</sup>	$f$	$0.142 \pm 0.03^{\dagger}$	$0.135^a$ $0.137^d$	$0.135^c$ $0.174^h$
	$\Gamma$	$144 \pm 8^{\dagger}$	$131^a$ $140^d$ $76^e$	$151^f$ $155^g$
$1s2s^22p^2 [^3P]^2P$				
C <sup>+</sup>	$f$	$0.10 \pm 0.03^{\ddagger}$	$0.135^a$	
	$\Gamma$	$59 \pm 6^{\ddagger}$	$56^a$ $62^b$	
N <sup>2+</sup>	$f$	$0.191 \pm 0.03^{\dagger}$	$0.220^a$	
	$\Gamma$	$58 \pm 7^{\dagger}$	$62^a$ $43^e$	$66^f$
O <sup>3+</sup>	$f$	$0.224 \pm 0.03^{\dagger}$	$0.200^a$ $0.253^d$	$0.243^c$ $0.318^h$
	$\Gamma$	$35 \pm 4^{\dagger}$	$75^a$ $67^d$ $76^f$	$78^f$ $92^g$
$1s2s^22p^2 [^1S]^2S$				
C <sup>+</sup>	$f$	$0.008 \pm 0.002^{\ddagger}$	$0.014^a$	
	$\Gamma$	$112 \pm 25^{\ddagger}$	$105^a$ $93^b$	
N <sup>2+</sup>	$f$	$0.014 \pm 0.005^{\dagger}$	$0.017^a$	
	$\Gamma$	$120 \pm 60^{\dagger}$	$106^a$ $94^e$	$132^f$
O <sup>3+</sup>	$f$	$0.043 \pm 0.02^{\dagger}$	$0.029^a$ $0.027^d$	$0.035^c$ $0.030^h$
	$\Gamma$	$26 \pm 22^{\dagger}$	$130^a$ $125^d$ $127^e$	$162^f$ $91^g$

<sup>†</sup>SOLEIL, experimental work.

<sup>‡</sup>ALS, experimental work [32].

<sup>a</sup>R-matrix, RMPS, 390 levels present work, <sup>b</sup>R-matrix, RMPS, 135 levels [32].

<sup>c</sup>CIV3. structure calculations, [35].

<sup>d</sup>R-matrix, [35], <sup>e</sup>R-matrix, optical potential [39].

<sup>f</sup>SCUNC, present work

<sup>g</sup>Saddle-point + complex rotation, [33].

<sup>h</sup>MCDF, present work.

namely,

$$f = 9.11 \times 10^{-3} \int_{E_1}^{E_2} \sigma(E) dE \quad (8)$$

where  $\sigma(E)$  is the photoionization cross section in Mb ( $1 \text{ Mb} = 1.0 \times 10^{-18} \text{ cm}^2$ ),  $E$  is the photon energy in eV, and  $E_1$  and  $E_2$  are the appropriate energy limits of the range for which the photoionization cross section is to be calculated.

Experimental and theoretical  $f$ -values were determined for the strong  $1s \rightarrow 2p$  core-excited resonances, resulting from 100% of the parent ion in the ground states for the first three members of the B-like sequence. The integrated oscillator strengths  $f$  (equation 8) are presented in figure 4 and numerical values in table 5 compared with other theoretical methods. We see from figure 4 and table 5 that the area under the peaks of the resonances for the R-matrix with pseudo-states (RMPS) 390-level approximation are in suitable agreement with the available experimental studies for all three ions. Similarly in figure 5, (for all three parent ions) and table 5 we present experimental and theoretical values (determined using a variety of methods) for the resonant Auger widths  $\Gamma$  (meV) of these same states. While there is satisfactory agreement between the R-matrix theoretical results and experiment for the integrated oscillator strength  $f$  along the isoelectronic sequence (as illustrated in figure 4) from figure 5, we see differences for the  $O^{3+}$  parent ion between theory and experiment for the resonance Auger widths of both the  $1s2s^22p^2 \ ^2P$  and  $1s2s^22p^2 \ ^2S$  core-excited states. The R-matrix with pseudo-states calculations (RMPS) and Saddle point calculations predict a monotonically increasing of the width for the three core-excited states, whereas in the case of the  $O^{3+}$  ion the present SOLEIL experiment show strong decreasing for the both the  $^2P$  and  $^2S$  resonance Auger states. Furthermore, from table 5 this behaviour is not supported by other theoretical methods for the same resonance widths of these Auger states, as consistency between the different state-of-the-art theoretical approaches (where electron correlation is satisfactory included) is found. The difference between theory and experiment for these two resonance is as yet unexplained so further independent investigation would be desirable to resolve this issue.

## 6. Conclusions

K-shell photoionization cross sections for B-like oxygen ions,  $O^{3+}$ , have been determined using state-of-the-art experimental and theoretical methods. High-resolution spectroscopy was able to be achieved with  $E/\Delta E = 5000$ , covering the energy range 540–630 eV. Several strong resonance peaks are found in the cross sections in the energy region 542–548 eV and 593–599 eV. These resonance peaks are identified as the  $1s \rightarrow 2p$  and  $1s \rightarrow 3p$  transitions in the  $O^{3+}$  K-shell spectrum and assigned spectroscopically with their resonance parameters tabulated in Tables 2, 3 and 4. For the observed resonance peaks, suitable agreement is found between the present theoretical and experimental results both on the photon-energy scale and on the absolute cross-section scale for this prototype B-like system. A comparison between theory and experiment for the integrated oscillator strengths  $f$  and Auger autoionization widths  $\Gamma$ , for the strong  $1s \rightarrow 2p$  resonances of the first few members of the B-like isoelectronic sequence highlight differences, particularly in the present experimental studies on the  $O^{3+}$  ion for the Auger widths of the  $1s2s^22p^2 \ ^2P$  and

$1s2s^22p^2$   $^2S$  core-excited states. These differences are as yet unexplained and would require further independent investigations.

The strength of the present study is the high resolution of the spectra along with theoretical predictions made using the state-of-the-art MCDF, R-matrix with pseudo-states methods and predictions from a semi-empirical approach. Cross section results from earlier R-matrix investigations (Garcia and co-workers [39], Pradhan and co-workers [36]) were restricted to the ground-state of this ion. The present results have been compared with high resolution experimental measurements made at the SOLEIL synchrotron radiation facility and with other theoretical methods so would be suitable to be incorporated into astrophysical modelling codes like CLOUDY [71, 72], XSTAR [73] and AtomDB [74] used to numerically simulate the thermal and ionization structure of ionized astrophysical nebulae.

### Acknowledgments

The experimental measurements were performed on the PLEIADES beam line, at the SOLEIL Synchrotron radiation facility in Saint-Aubin, France. The authors would like to thank the SOLEIL staff and, in particular C Miron the local contact of the PLEIADES beam line during the experiment for their helpful assistance. M F Gharaibeh acknowledges funding from the Scientific Research Support Fund, Jordan, for supporting a research visit to SOLEIL, under contract number Bas/2/02/2010. B M McLaughlin acknowledges support from the US National Science Foundation through a grant to ITAMP at the Harvard-Smithsonian Center for Astrophysics, the RTRA network *Triangle de la Physique* and a visiting research fellowship from Queen's University Belfast. We thank John C Raymond and Randall K Smith at the Harvard-Smithsonian Center for Astrophysics for discussions on the astrophysical applications. The computational work was carried out at the National Energy Research Scientific Computing Center in Oakland, CA, USA, the Kraken XT5 facility at the National Institute for Computational Science (NICS) in Knoxville, TN, USA and at the High Performance Computing Center Stuttgart (HLRS) of the University of Stuttgart, Stuttgart, Germany. Stefan Andersson from Cray Research is acknowledged for his advice and assistance with the implementation of the parallel R-matrix codes on the Cray-XE6 at HLRS. The Kraken XT5 facility is a resource of the Extreme Science and Engineering Discovery Environment (XSEDE), which is supported by National Science Foundation grant number OCI-1053575. This research also used resources of the Oak Ridge Leadership Computing Facility at the Oak Ridge National Laboratory, which is supported by the Office of Science of the U.S. Department of Energy under Contract No. DE-AC05-00OR22725.

### References

- [1] Ogle P M *et al* 2004 *Astrophys. J* **606** 151
- [2] Cassinelli J P *et al* 1981 *Astrophys. J* **250** 677
- [3] Blustin A J *et al* 2002 *Astron. and Astrophys.* **392** 453
- [4] Pérez-Montero E and Díaz A 2007 *Mon. Not. Roy. Astron. Soc.* **377** 1195
- [5] Smith J D T *et al* 2009 *Astrophys. J* **693** 713
- [6] Meléndez M *et al* 2008 *Astrophys. J* **682** 94
- [7] Liao Jin-Yuan *et al* 2013 *Astrophys. J* **774** 116
- [8] Pinto C *et al* 2013 *Astron. and Astrophys.* **551** 25
- [9] Gatuzz E *et al* 2013 *Astrophys. J* **768** 60
- [10] Gorczyca T W *et al* 2013 *Astrophys. J* **779** 78

- [11] Bruch R *et al* 1979 *Phys. Rev. A* **19** 587
- [12] Kawatsura K *et al* 2002 *J. Phys. B: At. Mol. Opt. Phys.* **35** 4147
- [13] Krause M O 1994 *Nucl. Instr. and Meth. in Phys. Res. B* **87** 178
- [14] Menzel A, Benzaid S, Krause M, Caldwell C D, Hergenhahn U and Bissen M 1996 *Phys. Rev. A* **54** R991
- [15] Stolte W C, Samson J A R, Hemmers O, Hansen D, Whitfield S B and Lindle D W 1997 *J. Phys. B: At. Mol. Opt. Phys.* **30** 4489
- [16] McLaughlin B M, Ballance C P, Bown K P, Gardenghi D J and Stolte W C 2013 *Astrophys. J* **771** L8
- [17] McLaughlin B M, Ballance C P, Bown K P, Gardenghi D J and Stolte W C 2013 *Astrophys. J* **779** L31
- [18] Vainshtein L A and Safronova U I 1978 *At. Data Nucl. Data Tables* **21** 49
- [19] Safronova U I and Shlyaptseva A S 1996 *Phys. Scr* **54** 254
- [20] Safronova U I, Shlyaptseva A S, Cornille M and Dubau J 1998 *Phys. Scr* **57** 395
- [21] Safronova U I and Shlyaptseva 1999 *Phys. Scr* **60** 36
- [22] Cornille M and Dubau J 1999 *Phys. Scr* **59** 27
- [23] Chen M H and Crasemann B 1987 *Phys. Rev A* **35** 4579
- [24] Chen M H and Crasemann B 1988 *At. Dat. Nucl. Data Tables* **38** 381
- [25] Chung C T and Bruch R 1983 *Phys. Rev. A* **28** 1418
- [26] Chung K T 1989 *Chin. J. Phys.* **27** 90
- [27] Chung K T 1990 *J. Phys. B* **23** 2929
- [28] Lin S-H, Hsue C-S and Chung K T 2001 *Phys. Rev. A* **64** 012709
- [29] Lin S-H, Hsue C-S and Chung K T 2002 *Phys. Rev. A* **65** 032706
- [30] Sun Y *et al* 2011 *J. Chem. Phys* **135** 124309
- [31] Bruch R *et al* 1985 *Phys. Rev. A* **31** 310
- [32] Schlachter A S, Sant'Anna M M, Covington A M, Aguilar A, Gharaibeh M F, Emmons E D, Scully S W J, Phaneuf R A, Hinojosa G, Álvarez I, Cisneros C, Müller A and McLaughlin B M 2004 *J. Phys. B: At. Mol. Opt. Phys.* **37** L103
- [33] Sun Y *et al* 2013 *Eur. Phys. J. D* **67** 88
- [34] Sun Y *et al* 2013 *Phys. Rev. A* **87** 032509
- [35] Zeng J and Yuan J 2002 *J. Phys. B: At. Mol. & Opt.* **35** 3054
- [36] Pradhan A K *et al* 2003 *Mon. Not. R. Astr. Soc.* **341** 1268
- [37] Burke P G and Berrington K A 1993 *Atomic and Molecular Processes: An R-matrix Approach* (Bristol, UK: IOP Publishing)
- [38] Petrini D 1981 *J. Phys. B: At. Mol.* **14** 3839
- [39] Garcia J *et al* 2005 *Astrophys. J Suppl. Ser.* **158** 68
- [40] Burke P G 2011 *R-Matrix Theory of Atomic Collisions: Application to Atomic, Molecular and Optical Processes* (New York, USA: Springer)
- [41] Sakho I *et al* 2013 *At. Data. Nuc. Data Tables* **99** 447
- [42] Sakho I *et al* 2013 *Phys. Scr.* **88** 035302
- [43] Gu M F *et al* 2005 *Astrophys. J* **627** 1066
- [44] Kaastra J 2005 private communication to M F Gu 2005
- [45] Mendoza C *et al* 2012 The Reliability of atomic data used for oxygen abundance determinations, Conference on Mapping Oxygen in the Universe, Instituto de Astrofísica de Canarias, May 14-18 URL <http://www.iac.es/congreso/oxygenmap/media/presentations/>
- [46] Gu M F 2010 private communication
- [47] Gharaibeh M F, Bizau J M, Cubaynes D, Guilbaud S, El Hassan N, Al Shorman M M, Miron C, Nicolas C, Robert E, Blancard C and McLaughlin B M 2011 *J. Phys. B: At. Mol. Opt. Phys.* **44** 175208
- [48] Al Shorman M M, Gharaibeh M F, Bizau J M, Cubaynes D, Guilbaud S, El Hassan N, Miron C, Nicolas C, Robert E, Sakho I, Blancard C and McLaughlin B M 2013 *J. Phys. B: At. Mol. Opt. Phys.* **46** 195701
- [49] Gharaibeh M F, El Hassan N, Al Shorman M M, Bizau J M, Cubaynes D, Guilbaud S, Blancard C and McLaughlin B M 2014 *J. Phys. B: At. Mol. Opt. Phys.* **47** 065201
- [50] Travnikova O *et al* 2010 *Phys. Rev. Letts.* **105** 233001
- [51] Miron C *et al* 2013 URL <http://www.synchrotron-soleil.fr/portal/page/portal/Recherche/LignesLumiere/PLEIADES>
- [52] Samson J A R 1967 *Techniques of Vacuum Ultraviolet Spectroscopy* (New York, USA: John Wiley & Sons)
- [53] Tanaka T *et al* 2008 *Phys. Rev. A* **78** 022516
- [54] Kato M *et al* 2007 *J. Electron Spectrosc. Relat. Phenom.* **160** 39

- [55] Kramida A E, Ralchenko Y, Reader J, and NIST ASD Team, 2014 NIST Atomic Spectra Database (version 5), National Institute of Standards and Technology, Gaithersburg, MD, USA URL [http://physics.nist.gov/PhysRefData/ASD/levels\\_form.html](http://physics.nist.gov/PhysRefData/ASD/levels_form.html)
- [56] Bruneau J 1984 *J. Phys. B: At. Mol. Phys.* **17** 3009
- [57] Ballance C P and Griffin D C 2006 *J. Phys. B: At. Mol. Opt. Phys.* **39** 3617
- [58] McLaughlin B M and Ballance C P 2012 *J. Phys. B: At. Mol. Opt. Phys.* **45** 085701
- [59] McLaughlin B M and Ballance C P 2012 *J. Phys. B: At. Mol. Opt. Phys.* **45** 095202
- [60] Clementi E and Roetti C 1974 *At. Data Nucl. Data Tables* **14** 177
- [61] Berrington K, Quigley L, and Zhang H L 1997 *J. Phys. B: At. Mol. & Phys.* **30** 5409
- [62] Hibbert A 1975 *Comput. Phys. Commun.* **9** 141
- [63] Petrini D and de Araújo F X 1997 *Astron. & Astrophys.* **326** 870
- [64] Fano U and Cooper J W 1968 *Rev. Mod. Phys.* **40** 441
- [65] Shore B W 1967 *Rev. Mod. Phys.* **39** 439
- [66] Wright J D *et al* 2008 *Phys. Rev. A* **77** 062512
- [67] Quigley L and Berrington K A 1996 *J. Phys. B: At. Mol. Phys.* **29** 4529
- [68] Quigley L, Berrington K A and Pelan J 1998 *Comput. Phys. Commun.* **114** 225
- [69] Ballance C P, Berrington K A and McLaughlin B M 1999 *Phys. Rev. A* **60** R4217
- [70] Cowan R D 1981 *The Theory of Atomic Structure and Spectra* (Berkeley, CA, USA: University of California Press)
- [71] Ferland G J, Korista K T, Verner D A, Ferguson J W, Kingdon J B and Verner E M 1998 *Pub. Astron. Soc. Pac.(PASP)* **110** 761
- [72] Ferland G J 2003 *Annu. Rev. Astron. Astrophys.* **41** 517
- [73] Kallman T R and Bautista M A 2001 *Astrophys. J. Suppl. Ser.* **134** 139
- [74] Foster A R, Ji L, Smith R K and Brickhouse N S 2012 *Astrophys. J* **756** 128